A Root-Music-Based Algorithm for Estimating the Axis Positions of Electromagnetic Transmitters

MUJAHID AL-AZZO, MUHAMMAD SALEM
Electronics Engineering Department,
Ninevah University,
Nineveh, Mosul,
IRAQ

Abstract: - The problem of determining the position of a wave radiation transmitter is important in the fields of communications and digital signal processing, where the transmitter's spatial position is specified with respect to a reference point. Spectral estimation methods differ in their characteristics, with the ability to distinguish between closely spaced transmitters being one of the most notable. This study focused on two methods: the Fourier Transform (FT) as a classical method and Root-MUSIC as a modern method. The positions of one and two transmitters were estimated under noisy and noise-free conditions, with the percentage error (E_{p_b}) in the position of each transmitter is calculated. The minimum separation (d_{p_t}), which represents the smallest distance at which two transmitters can be distinguished, was also calculated. Simulation results showed that Root-MUSIC outperforms the fast Fourier transform (FFT) in terms of accuracy in positioning and resolving the minimum distance between the transmitters.

Key-Words: - positioning estimation, Root-Music, Fourier transform, antenna array, super-resolution.

Received: March 7, 2025. Revised: June 19, 2025. Accepted: July 21, 2025. Published: November 25, 2025.

1 Introduction

The challenge of positioning wave radiation transmitters is considerable, especially in the fields of communications, digital signal processing (DSP), seismic technologies, sonar, radar, and medical sciences, [1], [2]. The precision of the positioning estimation method is the main factor on which these services depend. These applications heavily depend on the positions of radiating transmitters relative to spatially separated sensors. Such as the position of a mobile device transmitting a signal with respect to a reference point. For instance, advanced processing techniques can improve the quality of the received signal in wireless communication systems and lessen the impact of noise and interference, [3].

Data is recorded in time-varying quantities called signals, which can be either analog or discrete. These could be biological signals like heart electrical pulses, sonar or ultrasound signals, video signals, audio signals (music, speech), or a variety of different electromagnetic signals, [4]. After being received by the array antenna, the continuous-time signals are transformed into discrete signals for processing, [5].

In many applications, there is a need to receive signals and determine the number of incoming signals, which is particularly crucial in environments characterized by noise and interference. To accomplish this, an antenna array is employed, in which the sensing units are positioned linearly with equal distances separating them. This type of array is known as a uniform linear array (ULA), [6].

Understanding either the position of the signal's source or the direction of the source of the signal is necessary for array signal processing (ASP) to get the intended results, [1], [7], [8]. Typical ASP applications entail estimation of the direction of arrival (DOA), extraction of source position, and multipath problems in the presence of strong interference and noise, [9], [10]. ASP enhances the outputs of the sensors in antenna arrays to optimize system performance when compared to a single antenna. It has the advantages of increased signal-to-noise ratio (SNR), sidelobe (SL) control, and improved array resolution. ULA increases the received signal gain, [11].

Based on the application requirements, frequency estimation techniques, or spectral estimation in general, can be parametric (modern method) or nonparametric (classical method), [12], [13].

The classical methods made use of Cooley and Tukey's fast Fourier transform (FFT) in 1965. Despite their simplicity and speed of use, their precision is poor, and they suffer from side lobes (SL), which lowers the quality of the results. Moreover, noise sensitivity limits their effectiveness in noisy environments, [14], [15], [16].

High-resolution or subspace methods are branches of parametric methods, including the Root Multiple Signal Classification (Root-MUSIC or R-MUSIC) algorithm. They provide negligible SL levels, high resolution, and lower sensitivity to noise. The R-MUSIC method relies on polynomial roots analysis and offers super-resolution. The R-MUSIC algorithm usually does not present results as graphs, but gives outcomes in numbers, [17]. For a uniformly spaced linear array, the search for angles, closed frequencies, and positions can be performed by finding the roots of a polynomial using R-MUSIC, [8], [18].

2 Problem Formulation

An array is a collection of several sensors or antennas. An array element is a single sensor or antenna within the array. Spatial signals refer to the signals sent by transmitters in space or the signals received by the sensors. The ULA is a type of antenna array. It is composed of several elements placed in a straight line, with equal spacing, where the first element is positioned at the origin (reference axis). The distance between the elements is represented by Δ_t. The array has a total length of $(\eta-1)\,\Delta_t$, where η is the number of array elements. Figure 1 shows the geometry of a ULA with η elements (sensors), [19], [20].

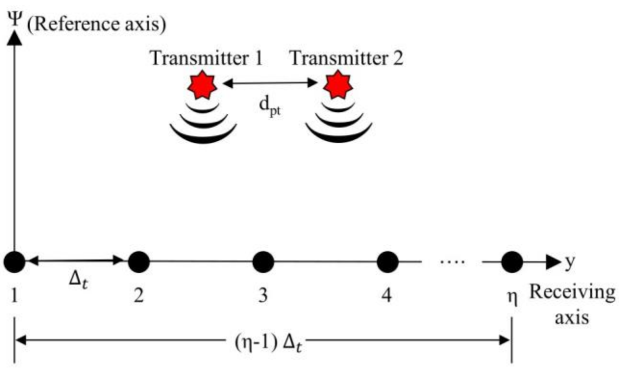

Fig. 1: Uniform linear array (ULA) coordinate system
Source: created by the authors

If there are L transmitters $q_1, q_2, ..., q_L$, where q_i represents the transmitter signal amplitude with $L < \eta$, then the detected or received signal y(n) for the η elements can be written in vector and matrix form, considering noise presence, as given by:

$$\boldsymbol{y}(n) = \boldsymbol{S}\,\mathbf{q}(n) + \boldsymbol{u}(n). \tag{1}$$

The signals received by all the η elements are organized into an $\eta\times1$ observation vector, represented as:

$$\boldsymbol{y} = [y_1, y_2, y_3, ..., y_\eta]^T. \tag{2}$$

where T denotes the transpose of a matrix or vector. **q** is the L×1 transmitting signal vector, as given below:

$$\mathbf{q} = [q_1, q_2, q_3, ..., q_L]^T. \tag{3}$$

Similarly, the observation noise vector, which has dimensions $\eta\times1$, is defined as [19], [20]:

$$\boldsymbol{u} = [u_1, u_2, u_3, ..., u_\eta]^T. \tag{4}$$

The array response matrix (or transmission matrix), denoted by **S**, is as follows:

$$\boldsymbol{S} = [\boldsymbol{s}(\phi_1), \boldsymbol{s}(\phi_2), \boldsymbol{s}(\phi_3), ..., \boldsymbol{s}(\phi_L)]. \tag{5}$$

$\mathbf{s}(\phi_i)$ denotes the signal's positioning vector with position p_{bi} of the ith transmitter for η elements and is defined as follows:

$$\boldsymbol{s}(\phi_i)=[1, \exp(-j\, 2\pi\, \Delta_t\, p_{bi} / z\, \lambda), \exp(-j\, 4\pi\, \Delta_t\, p_{bi} / z\lambda), ..., \exp(-j\, 2\pi\, \Delta_t\, p_{bi}\, (\eta - 1) / z\, \lambda)]^T. \tag{6}$$

where

$$\phi_i = \exp(-j\, 2\pi\, \Delta_t\, p_{bi} / z\, \lambda), \tag{7}$$

Δ_t is the sampling interval, p_{bi} is the position of the ith transmitter on the transmitting axis, z is the axial distance between the transmitting (T_X) and receiving (R_X) axes, and λ is the wavelength of the transmitting signal.

2.1 Classical Method (Fourier Transform)

The Discrete Fourier Transform (DFT) is one of the fundamental tools in signal analysis, as it relies on representing the signal using exponential functions with purely imaginary exponents. The DFT is distinguished as the only form of Fourier analysis that is discrete and finite in both time and frequency, making it suitable for digital applications and easy to implement on computers or digital devices. Thus, the DFT of a sequence y(n) with length η is given in [21], [22]:

$$Y(\alpha) = \sum_{n=0}^{\eta-1} y(n)\, \exp(-j\, 2\pi\, \alpha\, n / \eta). \tag{8}$$

Fourier analysis possesses the power preservation property, which means that power can be computed either in the time domain or the frequency domain, yielding the same result. Consequently, the DFT with a finite number of y(n) samples can be used to approximate the power spectral density (PSD) as:

$$P_{yy}(\alpha) = 1/\eta\, |\, Y(\alpha)\, |^2. \tag{9}$$

2.2 High-resolution Method (Root-Music)

The R-MUSIC algorithm is one of the subspace techniques and relies on the eigenstructure, which is similar to the multiple signal classification (MUSIC) algorithm but differs in the estimation approach. In the MUSIC algorithm, searching for spectral peaks requires intensive computations, whereas R-MUSIC replaces this step with finding the zeros (roots) of a polynomial of degree 2(L−1), reducing computational complexity while maintaining high accuracy. This method analyzes the roots of the spectral polynomial based on the eigenvectors of the sensor correlation matrix. These extracted roots represent the estimation of the signals (transmitters), [23], [24]. The MUSIC method can be expressed as:

$$P_{music}\ (p_b) = 1\ /\ \boldsymbol{s}^H\ \boldsymbol{V}_u\ \boldsymbol{V}_u^H\ \boldsymbol{s}. \quad (10)$$

where H is the Hermitian and $\mathbf{V}_u = [\mathbf{v}_{L+1}, ..., \mathbf{v}_\eta]$ is the matrix containing the eigenvectors corresponding to the noise subspace, [25], [26].

The signal vector can be expressed as:

$$\boldsymbol{s} = [1, \exp(-j\ 2\pi\ \Delta_t\ p_b\ /\ z\ \lambda), \exp(-j\ 4\pi\ \Delta_t\ p_b\ /\ z\ \lambda), ..., \exp(-j\ 2\pi\ \Delta_t\ p_b\ (\eta - 1)\ /\ z\ \lambda)]^T. \quad (11)$$

Let $x = \exp(-j\ 2\pi\ \Delta_t\ p_b\ /\ z\ \lambda)$; then Eq. (11) can be written in algebraic form as:

$$\boldsymbol{s} = [1, x, x^2, ..., x^{\eta-1}]^T. \quad (12)$$

As mentioned earlier, when receiving a signal from a transmitter or transmitters, the following relationship is obtained:

$$P_{music}^{-1}\ (p_b) = Poly\ (p_b) = \boldsymbol{s}^H\ (\boldsymbol{V}_u\ \boldsymbol{V}_u^H)\ \boldsymbol{s}. \quad (13)$$

where:

$$P_{music}^{-1}\ (p_b) = 1\ /\ P_{music}\ (p_b). \quad (14)$$

Let $\mathbf{D} = \mathbf{V}_u.\mathbf{V}_u^H$. In order to find the roots, P_{music}^{-1} (p_b) must be equal to zero, i.e., [27], [28],

$$P_{music}^{-1}\ (p_b) = Poly\ (p_b) = \boldsymbol{s}^H\ \boldsymbol{D}\ \boldsymbol{s} = 0. \quad (15)$$

Substituting (12) into (15) yields:

$$Poly\ (p_b) = \sum_{m=1}^{\eta} \sum_{k=1}^{\eta} x^k\ \boldsymbol{D}_{mk}\ x^{-m} = 0 \quad (16)$$

or

$$Poly\ (p_b) = \sum_{m=1}^{\eta} \sum_{k=1}^{\eta} \boldsymbol{D}_{mk}\ x^{k-m} = 0 \quad (17)$$

To simplify the final double summation, set $\ell = k - m$ to reduce it to a single sum, as shown below:

$$P_{R\text{-}music}\ (p_b) = \sum_{\ell=-(\eta-1)}^{\eta-1} \boldsymbol{D}_\ell\ x^\ell = 0. \quad (18)$$

where $\mathbf{D}_\ell = \sum_{\ell = k - m} \boldsymbol{D}_{mk}$.

Eq. (18) represents a polynomial of degree 2(L-1), which contains L-1 pairs of zeros. The zeros are distributed such that one is inside the unit circle (i.e., its magnitude is less than 1) and the other is outside. The roots are functions of transmitters' positions. This is clear from Eq. (7) and Eq. (12); hence, the positions could be determined from the roots.

3 Simulation Results

This paper presents simulation results for estimating the position of radiating transmitters, considering both single and dual transmitters, with and without noise. To achieve this, the classical FFT method and the modern method (super-resolution method), namely R-MUSIC, were utilized. All simulations were implemented in MATLAB.

The position of the transmitter is identified with respect to a reference point. Several parameters are used. p_{b1} and p_{b2} represent the positions of the first and second transmitters, respectively. λ denotes the wavelength, Δ_t represents the distance between antennas, and z indicates the distance between the T_X and R_X axes. All parameter units are in centimeters (cm). η corresponds to the number of antennas.

3.1 Error and Minimum Separation Criteria Definition

1- The percentage error (E_{p_b}) in the transmitter position is calculated by using the formula:

$$E_{p_b} = \frac{|p_b\ (\text{actual}) - p_b\ (\text{reconstructed})\ |}{p_b\ (\text{actual})} * 100\% \quad (19)$$

where p_b (actual) is the actual position of the transmitter, and p_b (reconstructed) is the estimated position after processing the received data by applying the method.

2- The minimum separation (d_{pt}) is calculated when there are two transmitters, representing the smallest distance between the transmitters that the method distinguishes between them and determines their positions.

The d_{pt} is calculated using the following equation:

$$d_{p_t} = p_{b_2} - p_{b_1} \quad (20)$$

In order to calculate the minimum separation between the two transmitters, the following procedures are followed:

a- Fixing the first transmitter, p_{b1}, in its position.

b- Moving the second position, p_{b2}, toward the first one until a certain criterion is reached.

  i- In the FFT algorithm, a number of sidelobes appear. The most dominant and important sidelobe is that which appeared between the two peaks that correspond to the two transmitters (in general, these peaks are of equal value since they were proposed to be equal in simulation). When the second transmitter's position becomes very close to the first one, the peak of the dominant sidelobe increases in its value. A criterion of -3 dB between the transmitter peak and the sidelobe is selected. So as long as the criteria are not reached, the moving of the second transmitter is continued and stopped when reaching this criterion. This separation between the two transmitters is regarded as a minimum separation that the algorithm could resolve (distinguish).

ii- In the R-MUSIC algorithm, the second transmitter's position is moved towards the first one until the E_{pb} is still considerably less than that of the FFT algorithm, such that it does not exceed 12.5% of R-MUSIC.

3.2 Single Transmitter Position Estimation without Noise

The position estimation of a single transmitter was studied using the following parameters: p_{b_1} = 2 cm, λ = 0.3 cm, Δ_t = 2 cm, z = 50 cm, and η = 7. Figure 2 shows the implementation of the FFT method. Using the FFT method, the estimated transmitter position is p_{b_1} = 2.0215 cm with E_{p_b} = 1.07% and observed sidelobes. In contrast, the R-MUSIC method was implemented, which provides a direct estimation of the transmitter position as a numerical value after processing. Using R-MUSIC, the estimated value of p_{b_1} is 2 cm with E_{p_b} = 0%.

The results indicated that this estimated value precisely matches the actual transmitter position, achieving the lowest E_{pb} and negligible SL, all of which enhance its accuracy in transmitter position estimation.

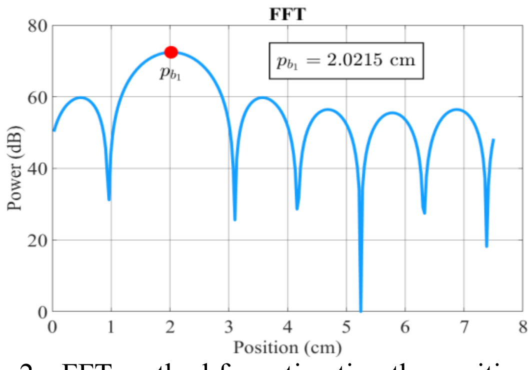

Fig. 2: FFT method for estimating the position of a single transmitter when p_{b_1} = 2 cm, λ = 0.3 cm, Δ_t = 2 cm, z = 50 cm, and η = 7
Source: created by the authors

Table 1 presents a comparison of the percentage error (E_{pb}) between the FFT and R-MUSIC methods, using a set of parameters.

Table 1. A percentage error (E_{p_b}) for FFT and R-MUSIC methods with λ = 0.3 cm, Δ_t = 2 cm, and η = 7

Parameters	E_{pb}	
	FFT	R-MUSIC
p_{b_1} = 2 cm, z = 50 cm	1.07%	0%
p_{b_1} = 2 cm, z = 70 cm	2.54%	0%
p_{b_1} = 4.5 cm, z = 50 cm	0.91%	0%
p_{b_1} = 4.5 cm, z = 70 cm	1.17%	0%

Source: created by the authors

Figure 3 and Figure 4 illustrate the results of applying the FFT and R-MUSIC methods for estimating the position of a single transmitter in a noise-free environment. The figures show the relationship between E_{pb} and η for the cases p_{b1} = 2 cm and p_{b1} = 4.5 cm, respectively, with the same other parameters. The results indicate that E_{pb} remains constant regardless of changes in η, and the R-MUSIC method achieves a significantly lower E_{pb} compared to the FFT method, with E_{p_b} = 0%. Additionally, it was observed that increasing z results in an increase in E_{pb} for the FFT method only. Moreover, it was observed that increasing p_{b1} to 4.5 cm leads to a reduction in E_{p_b} compared to the case when p_{b_1} = 2 cm.

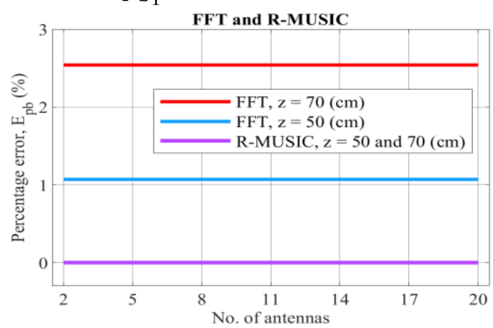

Fig. 3: Comparison of E_{p_b} and η for p_{b_1} = 2 cm, λ = 0.3 cm, and Δ_t = 2 cm
Source: created by the authors

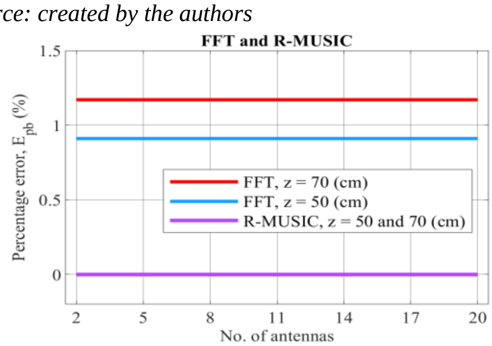

Fig. 4: Relationship between E_{p_b} and η for p_{b_1} = 4.5 cm, λ = 0.3 cm, and Δ_t = 2 cm
Source: created by the authors

3.3 Two Transmitters' Position Estimation without Noise

The estimation of the two transmitters' positions was studied using the following parameters: $p_{b_1} = 2$ cm, while p_{b_2} was varied to determine the minimum distinguishable distance between the two transmitters (d_{p_t}). The other parameters used were $\lambda = 0.3$ cm, $\Delta_t = 2$ cm, $z = 50$ cm, and $\eta = 7$. Figure 5 shows the results of applying the FFT method. The FFT method estimated the transmitters' positions at $p_{b_1} = 1.8164$ cm and $p_{b_2} = 3.1055$ cm, with the minimum distinguishable distance recorded as $d_{p_t} = 0.88$ cm and $E_{p_{b_1}} = 9.18\%$ with clear sidelobes. When the R-MUSIC method was implemented, it estimated the positions of two transmitters at $p_{b_1} = 1.9999$ cm and $p_{b_2} = 2.02$ cm, with $d_{p_t} = 0.02$ cm and $E_{p_{b_1}} = 0\%$.

The results indicate that R-MUSIC achieves superior performance, offering more precise transmitter position estimation with negligible SL, lower d_{pt}, and E_{pb} values compared to the previous method.

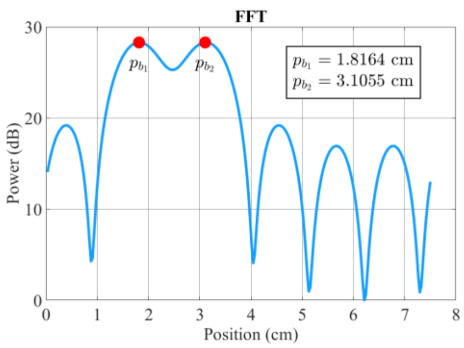

Fig. 5: FFT method for estimating the position of two transmitters when $p_{b_1} = 2$ cm, with p_{b_2} varied to determine d_{p_t}, $\lambda = 0.3$ cm, $\Delta_t = 2$ cm, $z = 50$ cm, and $\eta = 7$
Source: created by the authors

Table 2 presents a comparison of the minimum separation (d_{pt}) between the FFT and R-MUSIC methods using a set of parameters.

Table 2. A minimum separation (d_{pt}) for FFT and R-MUSIC methods with $\lambda = 0.3$ cm, $\Delta_t = 2$ cm, and $\eta = 7$

Parameters	Minimum d_{pt}	
	FFT	R-MUSIC
$p_{b_1} = 2$ and 4.5 cm, z = 50 cm	0.88 cm	0.02 cm
$p_{b_1} = 2$ and 4.5 cm, z = 70 cm	1.2322 cm	0.06 cm

Source: created by the authors

Table 3 presents a comparison of the E_{pb} between the FFT and R-MUSIC methods using a set of parameters.

Table 3. A percentage error (E_{p_b}) between FFT and R-MUSIC methods with $\lambda = 0.3$ cm, $\Delta_t = 2$ cm, and $\eta = 7$

Parameters	E_{pb}	
	FFT	R-MUSIC
$p_{b_1} = 2$ cm, z = 50 cm	9.18%	0%
$p_{b_1} = 2$ cm, z = 70 cm	11.82%	0%
$p_{b_1} = 4.5$ cm, z = 50 cm	4.30%	0%
$p_{b_1} = 4.5$ cm, z = 70 cm	5.21%	0%

Source: created by the authors

Figure 6 illustrates a comparison of d_{pt} and η after applying the FFT and R-MUSIC methods to estimate the positions of two transmitters in a noise-free environment. The results show that the R-MUSIC achieves the lowest d_{pt} value, very close to zero, indicating its high accuracy in distinguishing between very closely spaced transmitters. In contrast, the FFT records a significantly higher d_{pt} value. Additionally, it is observed that as z increases, d_{pt} increases, implying that a greater separation is required to distinguish between the transmitters. Furthermore, increasing p_{b1} from 2 cm to 4.5 cm results in the same minimum d_{pt} value for both R-MUSIC and FFT methods. It is observed that, as η increases, d_{pt} begins to decrease in the FFT method.

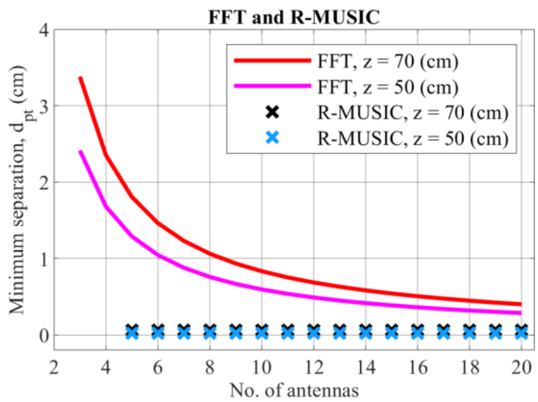

Fig. 6: Relationship between d_{p_t} and η for $p_{b_1} = 2$ and 4.5 cm, with p_{b_2} varied to determine d_{p_t}, $\lambda = 0.3$ cm, and $\Delta_t = 2$ cm
Source: created by the authors

Figure 7 and Figure 8 illustrate the relationship between E_{pb1} and η after implementing the FFT and R-MUSIC methods to estimate the positions of two transmitters in a noise-free environment (without noise) for the cases $p_{b1} = 2$ cm and $p_{b1} = 4.5$ cm, respectively, with the same other parameters. The results show that the R-MUSIC method achieves the lowest E_{pb1} value, reaching 0%, while the FFT method records considerably higher values, especially for $\eta \leq 6$. Additionally, it was observed that increasing z results in an increase in E_{pb1} for the FFT method only. Also, as η increases, E_{pb1} begins to decrease. Finally, the results show that increasing the value of p_{b_1} to 4.5 cm leads to a reduction in $E_{p_{b_1}}$ compared to the case when p_{b_1} = 2 cm for the FFT method.

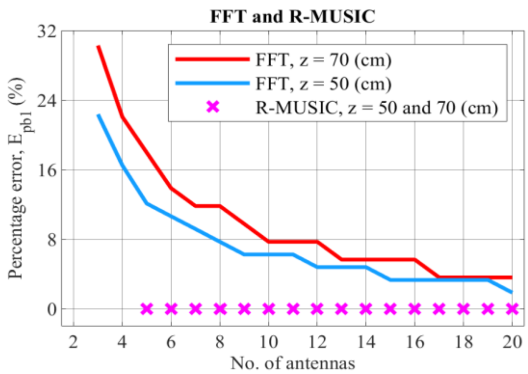

Fig. 7: Relationship between $E_{p_{b_1}}$ and η for p_{b_1} = 2 cm, with p_{b_2} varied to determine d_{p_t}, λ = 0.3 cm, and Δ_t = 2 cm
Source: created by the authors

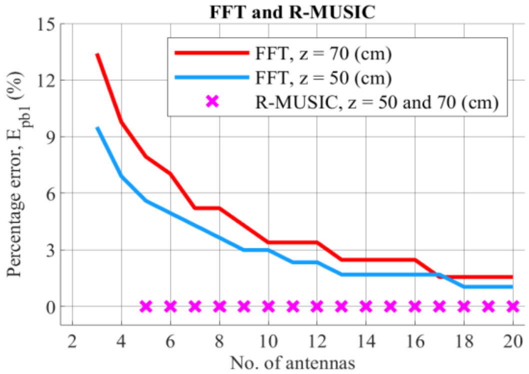

Fig. 8: Relationship between $E_{p_{b_1}}$ and η for p_{b_1} = 4.5 cm, with p_{b_2} varied to determine d_{p_t} , λ = 0.3 cm, and Δ_t = 2 cm
Source: created by the authors

3.4 Single Transmitter Position Estimation with Noise

When a signal is transmitted from T_X and received at R_X, it is affected by additive white Gaussian noise (AWGN). This noise is added to the original transmitted signal, and its impact on the results is examined.

The estimation of a single transmitter position is studied using the following parameters: p_{b_1} = 2 cm, λ = 0.3 cm, Δ_t = 2 cm, z = 50 cm, SNR = 10 dB, and η = 7. Figure 9 indicates the implementation of the FFT method. The results show that the FFT method estimated the transmitter position at p_{b_1} = 2.0215 cm with E_{p_b} = 1.07% with observed sidelobes. When the R-MUSIC method was implemented, it estimated the transmitter position at p_{b_1} = 2.0149 cm with E_{p_b} = 0.75%. Hence, its achievement is better, clearly, than the FFT method.

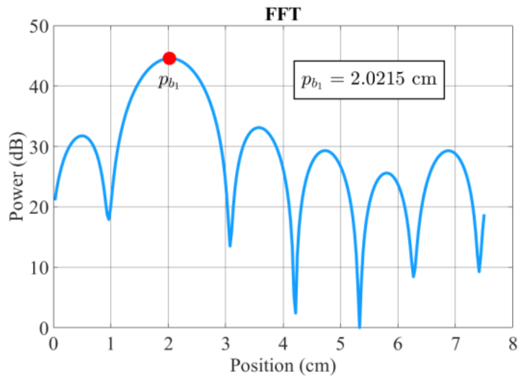

Fig. 9: FFT method for estimating the position of a single transmitter when p_{s_1} = 2 cm, λ = 0.3 cm, Δ_t = 2 cm, z = 50 cm, SNR = 10 dB, and η = 7
Source: created by the authors

Table 4 presents a comparison of the Epb between the FFT and R-MUSIC methods using a set of parameters.

Table 4. A percentage error (E_{p_b}) for FFT and R-MUSIC methods with λ = 0.3 cm, Δ_t = 2 cm, and η = 7

Parameters	E_{pb}	
	FFT	R-MUSIC
p_{b_1} = 2 cm, z = 50 cm, and SNR = 10 dB	1.07%	0.75%
p_{b_1} = 2 cm, z = 50 cm, and SNR = 5 dB	6.93%	2.68%
p_{b_1} = 2 cm, z = 70 cm, and SNR = 10 dB	4.59%	3.12%
p_{b_1} = 2 cm, z = 70 cm, and SNR = 5 dB	4.59%	3.12%
p_{b_1} = 4.5 cm, z = 50 cm, and SNR = 10 dB	1.56%	0.33%
p_{b_1} = 4.5 cm, z = 50 cm, and SNR = 5 dB	2.21%	0.57%
p_{b_1} = 4.5 cm, z = 70 cm, and SNR = 10 dB	2.99%	1.19%
p_{b_1} = 4.5 cm, z = 70 cm, and SNR = 5 dB	2.08%	1.24%

Source: created by the authors

Figure 10 and Figure 11 illustrate the relationship between E_{pb} and the parameter η after applying the FFT and R-MUSIC methods to estimate the position of a single transmitter in a noisy environment with p_{b_1} = 2 cm for both z = 50 cm and z = 70 cm, respectively, with different SNRs. The results indicate that increasing η contributes to a reduction in E_{pb}. Moreover, the results for z = 50 cm are better than those of 70 cm. A lower SNR results in an observed higher E_{pb} as compared with the noise-free environment case.

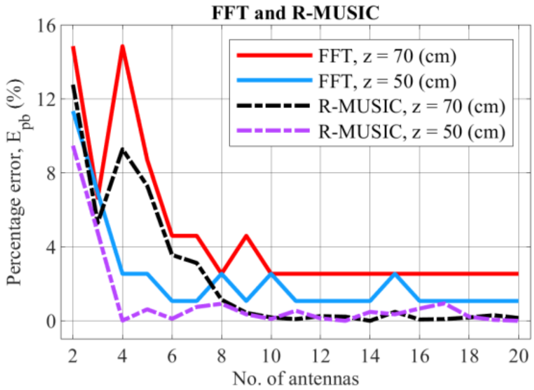

Fig. 10: Relationship between E_{p_b} and η for p_{b_1} = 2 cm, λ = 0.3 cm, SNR = 10 dB, and Δ_t = 2 cm

Source: created by the authors

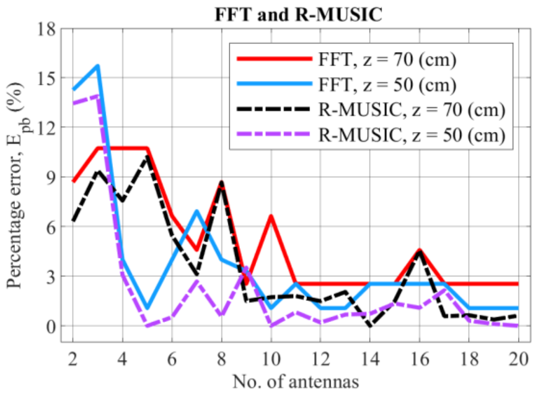

Fig. 11: Relationship between E_{p_b} and η for p_{b_1} = 2 cm, λ = 0.3 cm, SNR = 5 dB, and Δ_t = 2 cm

Source: created by the authors

Figure 12 and Figure 13 illustrate the relationship between E_{p_b} and the parameter η after applying the FFT and R-MUSIC methods to estimate the position of a single transmitter in a noisy environment with p_{b_1} = 4.5 cm for both z = 50 cm and z = 70 cm, respectively. The results show that increasing the value of p_{b_1} to 4.5 cm leads to a reduction in E_{p_b} compared to the case when p_{b_1} = 2 cm. Also, it is clear that the achievement for z = 50 cm is better than that of z = 70 cm.

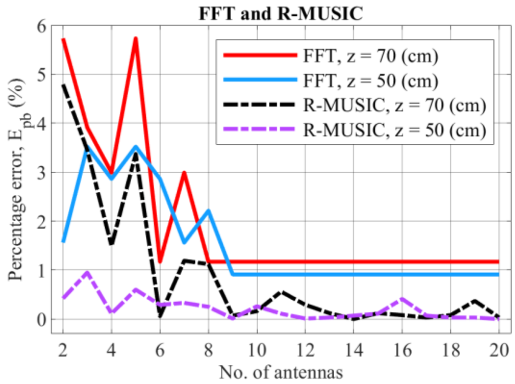

Fig. 12: Relationship between E_{p_b} and η for p_{b_1} = 4.5 cm, λ = 0.3 cm, SNR = 10 dB, and Δ_t = 2 cm

Source: created by the authors

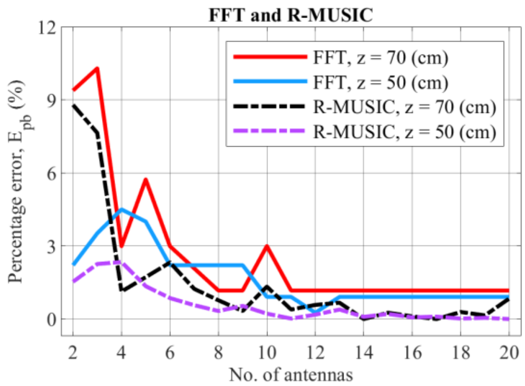

Fig. 13: Relationship between E_{p_b} and η for p_{b_1} = 4.5 cm, λ = 0.3 cm, SNR = 5 dB, and Δ_t = 2 cm

Source: created by the authors

3.5 Two Transmitters' Position Estimation with Noise

The estimation of the positions of two transmitters was studied using the following set of parameters: p_{b_1} = 2 cm, with a varying value of p_{b_2}, λ = 0.3 cm, Δ_t = 2 cm, z = 50 cm, SNR = 10 dB, and η = 7. Figure 14 indicates the results of applying the FFT method to estimate the transmitters' positions under the same noise conditions. The results showed that the FFT method estimated the transmitters' positions at p_{b_1} = 1.8164 cm and p_{b_2} = 3.1348 cm, with d_{p_t} = 0.9 cm and $E_{p_{b_1}}$ = 9.18%. When the R-MUSIC method was applied, it estimated the transmitters' positions at p_{b_1} = 2.088 cm and p_{b_2} = 2.348 cm, with d_{p_t} = 0.6 cm and $E_{p_{b_1}}$ = 4.4%. Hence, its achievement is better, clearly, than the FFT method.

Table 5 presents a comparison of the d_{pt} between the FFT and R-MUSIC methods using a set of parameters.

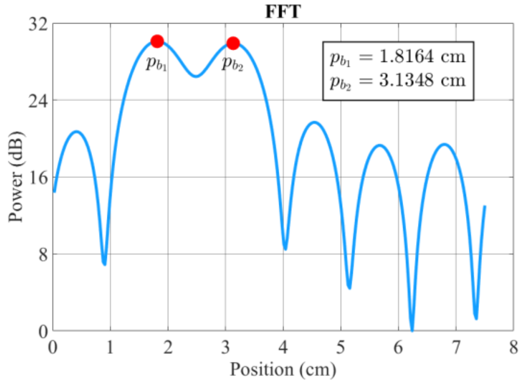

Fig. 14: FFT method for estimating the position of two transmitters when p_{b_1} = 2 cm, with p_{b_2} varied to determine d_{p_t}, λ = 0.3 cm, Δ_t = 2 cm, z = 50 cm, SNR = 10 dB, and η = 7

Source: created by the authors

Table 5. A minimum separation (d_{pt}) between FFT and R-MUSIC with λ = 0.3 cm, Δ_t = 2 cm, and η = 7

Parameters	Minimum d_{pt}	
	FFT	R-MUSIC
p_{b_1} = 2 cm, z = 50 cm, and SNR = 10 dB	0.9 cm	0.6 cm
p_{b_1} = 2 cm, z = 50 cm, and SNR = 5 dB	1.01 cm	0.81 cm
p_{b_1} = 2 cm, z = 70 cm, and SNR = 10 dB	1.26 cm	0.94 cm
p_{b_1} = 2 cm, z = 70 cm, and SNR = 5 dB	1.31 cm	0.8 cm

Source: created by the authors

Table 6 presents a comparison of the E_{pb} between the FFT and R-MUSIC methods using a set of parameters.

Table 6. A percentage error (E_{p_b}) for FFT and R-MUSIC method with λ = 0.3 cm, Δ_t = 2 cm, and η = 7

Parameters	E_{pb}	
	FFT	R-MUSIC
p_{b_1} = 2 cm, z = 50 cm, and SNR = 10 dB	9.18%	4.4%
p_{b_1} = 2 cm, z = 50 cm, and SNR = 5 dB	10.64%	4.01%
p_{b_1} = 2 cm, z = 70 cm, and SNR = 10 dB	11.82%	8.56%
p_{b_1} = 2 cm, z = 70 cm, and SNR = 5 dB	15.92%	12.31%

Source: created by the authors

Figure 15 and Figure 16 illustrate the relationship between d_{pt} and the parameter η, following the application of the FFT and R-MUSIC methods for estimating the positions of two transmitters in a noisy environment. The results indicate that an increase in z leads to a higher value of d_{p_t} for SNR = 10 dB and SNR = 5 dB, respectively. Additionally, a decrease in SNR causes an increase in d_{pt}. Finally, as η increases, a gradual decrease in d_{pt} is observed. The results show that the R-MUSIC achieves the lowest d_{pt} value, indicating its high accuracy in distinguishing between very closely spaced transmitters.

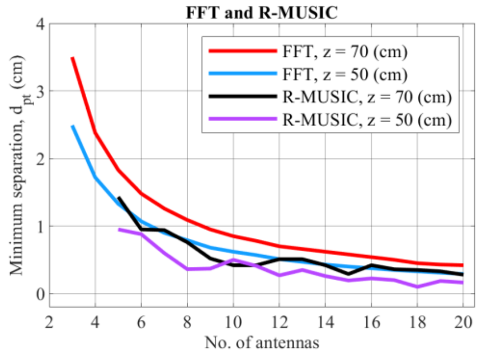

Fig. 15: Relationship between d_{p_t} and η for p_{b_1} = 2 cm, with p_{b_2} varied to determine d_{p_t}, λ = 0.3 cm, Δ_t = 2 cm, and SNR = 10 dB

Source: created by the authors

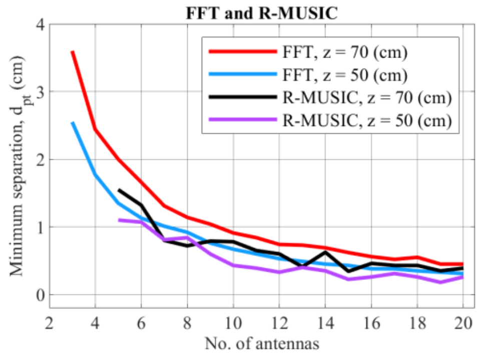

Fig. 16: Relationship between d_{p_t} and η for p_{s_1} = 2 cm, with p_{b_2} varied to determine d_{p_t}, λ = 0.3 cm, Δ_t = 2 cm, and SNR = 5 dB

Source: created by the authors

Figure 17 and Figure 18 illustrate the relationship between E_{pb1} and the parameter η after applying the FFT and R-MUSIC methods to estimate the positions of two transmitters in a noisy environment. The findings indicate that decreasing SNR increases E_{pb1} for low values of η. Moreover, as η increases, a gradual decrease in E_{pb1} is observed. The R-MUSIC method has a clearly better achievement for lower values of η.

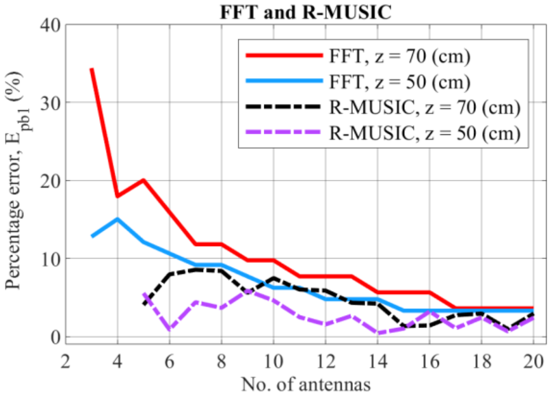

Fig. 17: Relationship between $E_{p_{b_1}}$ and η for p_{b_1} = 2 cm, with p_{b_2} varied to determine d_{p_t}, λ = 0.3 cm, Δ_t = 2 cm, and SNR = 10 dB

Source: created by the authors

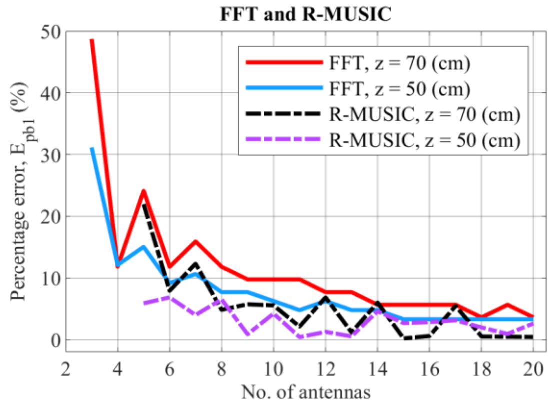

Fig. 18: Relationship between $E_{p_{b_1}}$ and η for p_{b_1} = 2 cm, with p_{b_2} varied to determine d_{p_t}, λ = 0.3 cm, Δ_t = 2 cm, and SNR = 5 dB

Source: created by the authors

4 Conclusion

In this paper, the performance of the modern high-resolution method, also called the super-resolution method (Root-MUSIC), was studied and compared with the classical method (FFT) for estimating the position of one and two transmitters relative to a reference point, both in the presence and absence of noise. Several parameters were used to study their effect on the performance of the mentioned methods, namely, p_{b1}, p_{b2}, z, and η. In addition, both d_{pt}, which represents the smallest separation between the transmitters that the method distinguishes between and determines their positions, and E_{pb}, which represents the error in transmitter position estimation, were calculated.

The FFT method is characterized by its simplicity; however, it suffers from poor accuracy in the transmitter's position estimation, especially when the transmitters are very close to each other. It also exhibits high SL levels and has a wide peak. On the other hand, the modern method (Root-MUSIC) is distinguished by its high accuracy in estimating transmitter positions even when they are close to each other, with no SL levels. Although this method involves more computational complexity, this does not pose a significant challenge due to the speed and advancement of modern computers.

The simulation results, in the absence of noise, showed that the R-MUSIC method is the most accurate in estimating transmitters' positions, achieving the lowest E_{pb} value of 0% and the smallest d_{pt}, with values very close to zero. In contrast, the highest values of E_{pb} and d_{pt} were recorded using the FFT method.

In the presence of noise, the R-MUSIC method also outperformed the FFT for different parameters. Hence, the R-MUSIC method showed higher achievement than the FFT method.

The contribution of the work is to deal with high-frequency signals (75 - 100 GHz) and the modeling of the transmitters' positioning problem for the R-MUSIC method. Also, the errors (E_{pb}, d_{pt}) are decreased as the distance of the first (nearest) transmitter from the reference axis increases.

The transmitters' positioning estimation problem could be applied to problems of mobile devices' positioning with respect to some reference axis, and also to the civil rescue problem.

Declaration of Generative AI and AI-assisted Technologies in the Writing Process

The authors wrote, reviewed and edited the content as needed and verifies that none utilized artificial intelligence (AI) tools were used. The authors take full responsibility for the content of the publication.

References:

[1] I. Sharp and K. Yu, Wireless Positioning: Principles and Practice. In Navigation: Science and Technology. Singapore: Springer Singapore, 2019.

[2] A. A. Salama, "Compressive Sensing Based Estimation of Direction of Arrival in Antenna Arrays," PhD Thesis, Concordia University, Montreal, Canada, 2017.

[3] M. A. Al-Sadoon, "Direction Finding and Beamforming Techniques using Antenna Array for Wireless System Applications," PhD Thesis, University of Bradford, 2019.

[4] B. G. Liptak et al., Instrument engineers' handbook, volume two: Process control and optimization. CRC Press, 2018.

[5] S. Mohammadi, A. Ghani, and S. H. Sedighy, "Direction-of-arrival estimation in conformal microstrip patch array antenna," *IEEE Trans. Antennas Propag.*, vol. 66, no. 1, pp. 511–515, 2017. https://doi.org/10.1109/TAP.2017.2772085.
[6] K. Raghu, "Performance evaluation & analysis of direction of arrival estimation algorithms using ULA," in *2018 International Conference on Electrical, Electronics, Communication, Computer, and Optimization Techniques (ICEECCOT)*, Mysuru, India: IEEE, 2018, pp. 1467–1473.
[7] J. Benesty, I. Cohen, and J. Chen, Fundamentals of signal enhancement and array signal processing. John Wiley & Sons, 2017. doi: 10.1002/9781119293132.
[8] L. Osman, I. Sfar, and A. Gharsallah, "The application of high-resolution methods for DOA estimation using a linear antenna array," *Int. J. Microw. Wireless. Technol.*, vol. 7, no. 1, pp. 87–94, 2015. https://doi.org/10.1017/S1759078714000464.
[9] A. L. Swindlehurst, B. D. Jeffs, G. Seco-Granados, and J. Li, "Applications of array signal processing," in *Academic Press Library in Signal Processing*, vol. 3, Elsevier, 2014, pp. 859–953.
[10] A. Argyriou, "Number of sources detection and AoA estimation of a wireless transmitter in multipath channels," in *2022 3rd URSI Atlantic and Asia Pacific Radio Science Meeting (AT-AP-RASC)*, Gran Canaria, Spain: IEEE, 2022, pp. 1–4.
[11] Z. Ahmad, "Array Signal Processing," Adapt. Filter. *Recent Adv. Pract. Implement*, p. 3, 2021.
[12] M. V. Kraynyuk and O. K. Alsova, "Research of the synchronous spectral analysis method," in *2016 11th International Forum on Strategic Technology (IFOST)*, Novosibirsk, Russia: IEEE, 2016, pp. 449–450.
[13] T. Holton, Digital signal processing: Principles and applications. Cambridge University Press, 2021.
[14] H. Wen, S. Guo, Z. Teng, F. Li, and Y. Yang, "Frequency estimation of distorted and noisy signals in power systems by FFT-based approach," *IEEE Trans. Power Syst.*, vol. 29, no. 2, pp. 765–774, 2013. https://doi.org/10.1109/TPWRS.2013.2283273.
[15] O. Martinez Manzanera, J. W. Elting, J. H. van der Hoeven, and N. M. Maurits, "Tremor detection using parametric and non-parametric spectral estimation methods: A comparison with clinical assessment," *PloS One*, vol. 11, no. 6, p. e0156822, 2016. https://doi.org/10.1371/journal.pone.0156822.
[16] M. Behrendt, M. de Angelis, L. Comerford, Y. Zhang, and M. Beer, "Projecting interval uncertainty through the discrete Fourier transform: An application to time signals with poor precision," *Mech. Syst. Signal Process.*, vol. 172, p. 108920, 2022. https://doi.org/10.1016/j.ymssp.2022.108920.
[17] A. Koljonen, "Estimation of the Direction of Arrival of Sounding Reference Signal with Neural Networks," Master's thesis, Aalto University, Espoo, Finland, 2020.
[18] C. Liu, X. Cheng, J. Su, and Y. Yuan, "Research and Simulation of Super-resolution Root-MUSIC Algorithm," in *2023 4th International Symposium on Computer Engineering and Intelligent Communications (ISCEIC)*, Nanjing, China: IEEE, 2023, pp. 95–99. https://doi.org/10.1109/ISCEIC59030.2023.10271196.
[19] X.-D. Zhang, *Modern signal processing*. Walter de Gruyter GmbH & Co KG, 2022. https://doi.org/10.1515/9783110475562.
[20] W. Yang, *Sensor array*. BoD–Books on Demand, 2012.
[21] D. Sundararajan, *Digital Signal Processing: An Introduction*. Springer Nature, 2024. https://doi.org/10.1007/978-3-031-56740-7.
[22] K. S. Thyagarajan, Introduction to digital signal processing using MATLAB with application to digital communications. Springer, 2018. https://doi.org/10.1007/978-3-319-76029-2.
[23] M. A. Jatoi, N. Kamel, and S. H. A. Musavi, "Framework for estimating active brain sources using MUSIC and Root MUSIC," in *2017 International Conference on Innovations in Electrical Engineering and Computational Technologies (ICIEECT)*, Karachi, Pakistan: IEEE, 2017, pp. 1–6.
[24] A. Swaroop, Z. Polkowski, S. D. Correia, and B. Virdee, Eds., *Proceedings of Data Analytics and Management: ICDAM 2023*, Vol. 1, vol. 785. in Lecture Notes in Networks and Systems, vol. 785. London, United Kingdom, Singapore: Springer Nature Singapore, 2024.
[25] J. V. Candy, *Signal Processing: An Applied Decomposition Approach*. John Wiley & Sons, 2024. ISBN: 978-1-394-20746-6.

[26] J. B. Tsui, *Special design topics in digital wideband receivers*. Artech House, 2010. e-ISBN: 9781608070312.

[27] X. Wang, X. Wang, W. Zhai, and K. Cai, *Sparse Sensing and Sparsity Sensed in Multi-sensor Array Applications.* Singapore: Springer Nature Singapore, 2024. https://doi.org/10.1007/978-981-99-9558-5.

[28] A. Quinquis, Digital signal processing using MATLAB. Wiley-IEEE Press, 2008.

Contribution of Individual Authors to the Creation of a Scientific Article (Ghostwriting Policy)

The authors equally contributed in the present research, at all stages from the formulation of the problem to the final findings and solution.

Sources of Funding for Research Presented in a Scientific Article or Scientific Article Itself

No funding was received for conducting this study.

Conflict of Interest

The authors have no conflicts of interest to declare that are relevant to the content of this article.